วิศวกรรมสาร มข. ปีที่ 36 ฉบับที่ 2 (165-171) เมษายน – มิถุนายน 2552
KKU Engineering Journal Vol.36 No.2 (165-171) April – June 2009

Performance of Differential Detection with PSM versus BPM Signal for UWB Indoor Communication System over Multipath Channel

Chanyuth Chanatrirattanaphan[1] and Phichet Moungnoul[*2]

Abstract

In this paper, we analyzed the performance of differential detection with pulse shape modulation (PSM) versus bi-phase modulation (BPM) signal for ultra wide band (UWB) indoor communication system over multipath channel. The bit error rate (BER) performance of differential detection with PSM and BPM signal are investigated by using the IEEE 802.15.3a Saleh-Valenzuela (S-V) UWB multipath channel model. The data rate has been verified to be effective in overcoming the inter symbol interferences (ISI).

Keywords: PSM, BPM, UWB, Differential detection, S-V model

[1] Post graduated Students, Telecommunication Engineering, Faculty of Engineering, King Mongkut's Institute of Technology Ladkrabung, Bangkok 10520, E-mail: chanyuth.c@hotmail.com

[*2] Assistant Professor, Faculty of Engineering, King Mongkut's Institute of Technology Ladkrabung, Bangkok 10520

Introduction

Ultra wideband (UWB) radio signals employ the transmission of very short impulses of radio energy whose characteristic spectrum signature extends across a wide range of radio frequencies [1]. Much of the increased attention on UWB technology is due to the landmark ruling by the Federal Communications Commission (FCC). In February 2002, the FCC opened up 7,500 MHz of spectrum (from 3.1 GHz to 10.6 GHz) for UWB devices with a peak power-spectral-density (PSD) value of only -41.3dBm/MHz.

The differential detection approach can be a promising solution for attaining low-complexity and energy-efficient receivers. The differential detection is simpler to implement as they do not need channel estimation [3]. Assuming pulse shape modulation (PSM) in differential detection systems, the symbols are differentially encoded, and each received data pulse is correlated with the previous one. Each pulse serves as a template for the next.

In this paper, we analyzed and compared the performance of differential detection for UWB indoor communication system over multipath channel with orthogonal and antipodal signal which were represented by pulse shape modulation and bi-phase modulation (BPM) [1], respectively.

We present the PSM and BPM waveforms, PSM and BPM transmission, high frequency channel model by using Saleh-Valenzuela (S-V) model and the differential detection. Furthermore; we present all system simulation, simulation result and conclusions respectively.

System Models

PSM and BPM Waveforms

The UWB waveforms used for PSM scheme are the orthogonal pair of modulated Gaussian waveforms [2, 6-8]. The orthogonal pair of modulated Gaussian waveforms in time domain, f_0 and f_1 are given by

$$f_0(t) = A_0 e^{-(t/d)^2} \sin(2\pi f_c t) \tag{1}$$

$$f_1(t) = A_1 e^{-(t/d)^2} \cos(2\pi f_c t) \tag{2}$$

Where f_c is the carrier frequency, d is the $1/e$ characteristic decay time, A_0 and A_1 are the maximum amplitudes of waveform envelopes of f_0 and f_1, respectively.

PSM and BPM Transmission

The PSM and BPM transmission signals are denoted by $s_{PSM}(t)$ and $s_{BPM}(t)$ respectively, if $b(n)$ is binary input and $d(n)$ is Gray/Binary output, then

$$d(n)=d(n-1) \oplus b(n) \tag{3}$$

where $b(n) \in \{0,1\}$, $d(0)=b(0)$, $n = 0,1,2,...$

$$s_{PSM}(t)=\begin{cases} f_0(t) \text{ for } d(n)=0 \\ f_1(t) \text{ for } d(n)=1 \end{cases} \tag{4}$$

$$s_{BPM}(t)=\begin{cases} -f_1(t) \text{ for } d(n)=0 \\ f_1(t) \text{ for } d(n)=1 \end{cases} \tag{5}$$

The transmitted signals are given by $s(t) = s_{PSM}(t)$ of transmitted PSM signal sequence and $s(t) = s_{BPM}(t)$ of transmitted BPM signal sequence respectively.

High-Frequency Channel Model

The HF channel model has been established by the IEEE 802.15.3a standardization group for evaluating various proposals for high data rate UWB communication systems. This model is intended to represent the channel characteristics in the frequency range from 3.1 to 10.6 GHz. It is based on the Saleh-Valenzuela model [4], which represents a "clustering" of the paths. The channel impulse response is defined as

$$h_i(t) = X_i \sum_{l=0}^{L} \sum_{k=0}^{K} a_{k,l}^i \delta\left(t - T_l^i - \tau_{k,l}^i\right) \quad (6)$$

where $a_{k,l}^i$ is the tap weight associated with the k-th ray of the l-th cluster, X_i represents the log-normal shadowing, and i refers to the i-th realization; K is the number of rays in each cluster, and L is the number of clusters. The distributions of cluster and ray interarrival times, respectively, are given by

$$p_r\left(T_l \mid T_{l-1}\right) = \Lambda \exp\left[-\Lambda\left(T_l - T_{l-1}\right)\right], \quad l > 0$$
$$p_r\left(\tau_{k,l} \mid \tau_{k-1}, l\right) = \lambda \exp\left[-\lambda\left(\tau_{k,l} \mid \tau_{k-1,l}\right)\right], \; k > 0.$$

The channel coefficients are defined as $a_{k,l} = p_{k,l}\xi_l\beta_{k,l}$, where $p_{k,l} \in \{+1,-1\}$ is equiprobable and represents the signal inversion due to reflections. The parameter ξ_l reflects the fading associated with the l-th cluster, and $\beta_{k,l}$ corresponds to the fading associated with the k-th ray of the l-th cluster. The distribution of the channel coefficients is given by $\left|\xi_l\beta_{k,l}\right| = 10^{(\mu_{k,l}+n_1+n_2)/20}$, where $n_1 \sim N\left(0,\sigma_1^2\right)$ and $n_2 \sim N\left(0,\sigma_2^2\right)$ are independent Gaussian random variables corresponding to the fading of each cluster and ray, respectively. The parameters $\mu_{k,l}$ are given by

$$\mu_{k,l} = \frac{10\ln\left(\Omega_0\right) - 10T_l/\Gamma - 10\tau_{k,l}/\gamma}{In(10)} - \frac{\left(\sigma_1^2+\sigma_2^2\right)\ln(10)}{20} \quad (7)$$

Where Ω_0 is the mean energy of the first path in the first cluster, T_l and $\tau_{k,l}$ are the excess delays of cluster l and of the k-th ray in cluster l, respectively. Γ is the clusters' decay constant and γ is the rays' decay constant. Finally, the total energy contained in the terms $\left\{a_{k,l}^i\right\}$ is normalized to unity for each realization, because the lognormal shadowing of the total multipath energy is characterized by X_i, for $20\log_{10} X_i \sim N\left(0,\sigma_x^2\right)$. Based on the work of IEEE 802.15 also recommends a new way of modeling the path-loss. While there is still shadowing superimposed on a polynomial power decay law with the logarithm of distance, the decay exponent n and the shadowing variance σ^2 have now become random variables.

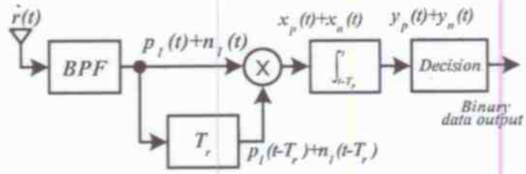

Figure 1: Differential detection

Differential Detection

In this section, the performance of the differential detection [3] in Figure 1 is analyzed with an integrator as shown. The input signal to the receiver is given by $r(t) = s(t)*h(t)+n(t)$, where $s(t)*h(t)$ is the received pulse waveform, and $n(t)$ is AWGN. The received signal is passed through a wideband bandpass filter that has the same impulse response as the transmitter filter, denoted by $h_B(t)$. Hence $p_I(t) = \left[s(t)*h(t)\right]*h_B(t)$ and

$$n_I(t) = n(t)*h_B(t) = \int n(\tau)h_B(t-\tau)\,d\tau \quad (8)$$

The noise process $n_I(t)$ has the autocorrelation given by

$$R_{n_In_I}(\tau) = \frac{N_0}{2}\int h_B(u)h_B(u-\tau)\,du \quad (9)$$

The receiver BPF output is multiplied with a replica delayed by T_r seconds and the resulting product decomposed into the components $x(t) = x_p(t) + x_n(t)$. Here $x_p(t) = p_I(t)\,p_I(t-T_r) = p_I^{\,2}(t)$, assuming that $p_I(t) = p_I(t-T_r)$ if the different bit input is sent.

$$x_n(t) = p_I(t)\left[n_i(t) + n_i(t-T_r)\right] + n_i(t)n_i(t-T_r) \quad (10)$$

The output of the mixer is integrated over a time period T_L, $0 < T_L \le T_r$ and a decision on the symbol is made every T_r sec. Thus, the output of the integrator, sampled at T_r spaced intervals, can be written as the sum of a signal component $y_p(T_L) = \int_0^{T_L} x_p(t)\,dt$, and a noise component $y_n(T_L) = \int_0^{T_L} x_n(t)\,dt = N_1 + N_2$, where $N_1 = \int_0^{T_L} p_I(t)\left[n_i(t) + n_i(t-T_r)\right]dt$, and $N_2 = \int_0^{T_L} n_i(t) n_i(t-T_r)\,dt$, $y_n(T_L)$ is no longer Gaussian due to the result of the term N_2. Rather than trying to derive the probability of error for the differential detection, the signal-to-noise ratio (SNR) at the output of the integrator is examined as a function of the integrator length T_L. The noise term $y_n(T_L)$ has a mean given by:

$$\begin{aligned} E\{y_n(T_L)\} &= E\{N_1\} + E\{N_2\} \\ &= \int_0^{T_L} p_I(t)\left[E\{n_i(t)\} + E\{n_i(t-T_r)\}\right]dt \\ &\quad + R_{n_in_i}(T_r)T_L \end{aligned} \quad (11)$$

Clearly, the first of these terms is zero, since $n_i(t)$ is a zero mean random process. The second is also approximately zero, if the impulse response of the BPF has negligible autocorrelation at lag T_r seconds, which holds in situations where the pulse repetition frequency of the UWB signal is small compared with the UWB signal bandwidth. Thus, $E\{y_n(T_L)\} \approx 0$. The variance of $y_n(T_L)$ is then given by

$$E\left\{y_n(T_L)^2\right\} \approx E\left\{N_1^2\right\} + E\left\{N_2^2\right\} + 2E\{N_1N_2\} \quad (12)$$

The first term on the right hand side can be written as

$$\begin{aligned} E\left\{N_1^2\right\} &= \iint_{T_L} p_I(t_1)\,p_I(t_2)\begin{pmatrix} 2R_{n_in_i}(t_1-t_2) \\ +R_{n_in_i}(t_1-t_2+T_r) \\ .R_{n_in_i}(t_1-t_2-T_r) \end{pmatrix} dt_1dt_2 \\ &= 2\iint_{T_L} p_I(t_1)\,p_I(t_2)\,R_{n_in_i}(t_1-t_2)\,dt_1dt_2 \end{aligned} \quad (13)$$

based on the previous discussion about $R_{n_in_i}(\tau)$.

Next,

$$\begin{aligned} E\left\{N_2^2\right\} &= \iint_{T_L} E\begin{Bmatrix} n_i(t_1)\,n_i(t_1-T_r) \\ .n_i(t_2)\,n_i(t_2-T_r) \end{Bmatrix} dt_1dt_2 \\ &= \iint_{T_L}\begin{bmatrix} R^2_{n_in_i}(T_r) + R^2_{n_in_i}(t_1-t_2) \\ +R_{n_in_i}(t_1-t_2+T_r)\,R_{n_in_i}(t_1-t_2-T_r) \end{bmatrix} dt_1dt_2 \\ &= \iint_{T_L} R^2_{n_in_i}(t_1-t_2)\,dt_1dt_2 \end{aligned} \quad (14)$$

where the well-known result for the fourth moment of jointly Gaussian variables has been used, and previous arguments about $R_{n_in_i}(\tau)$ have also been employed in the approximation. The final expression below in (15), along with (13) and (14), allows numerical computation of the output SNR for a given receiver BPF impulse response.

$$SNR_{out} = \frac{y_p^2(T_L)}{Var\left\{y_n^2(T_L)\right\}} = \frac{\left[\int_0^{T_L} p_I^{\,2}(t)\,dt\right]^2}{E\left\{N_1^2\right\} + E\left\{N_2^2\right\}} \quad (15)$$

From (15), we see that as the integration time is increased from zero, more signal energy is gathered, and the SNR_{out} increases initially. However, when the integration time extends past the pulse duration for an AWGN channel, no significant additional signal energy is gathered, while the noise terms, especially N_2, continue to accumulate, causing the SNR_{out} to decrease.

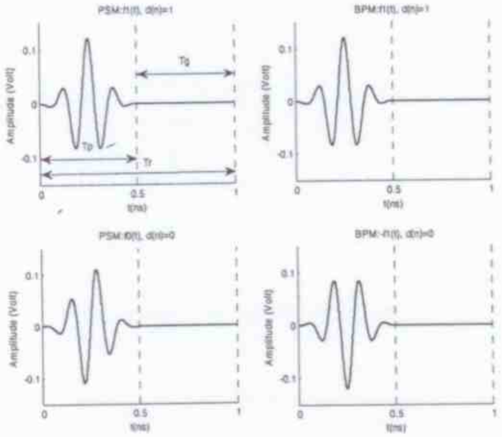

Figure 2: PSM and BPM signal with T_g =0.5ns

Simulation

UWB signal design

For the FCC indoor limit spectral mask, the waveform parameters are A_0 = A_1 =3.76V, d =0.11ns and f_c =7.34 GHz. The fractional bandwidth, occupied bandwidth and average power of these waveforms are 0.84, 6.20 GHz and -62.75dBm, respectively.

Sampling rate is 0.05ns, guard time (T_g) is related to the data rate of the transmitted signal and pulse time (T_p) is 0.5ns, where data rate of transmitted signal is $1/(T_p+T_g)$ bps. For the receiver, PSM bit decision threshold is 0.5 and BPM bit decision threshold is 0. Assume that the BPF is the imaginary bandpass filter by $h_B(t)$=1.

Table 1: S-V model parameters

Model Parameters	CM 1	CM 2	CM 3	CM 4
Λ (1/nsec)	0.0233	0.4	0.0667	0.0667
λ (1/nsec)	3.75	1	3	3
Γ	7.1	5.2	14.93	17
γ	4.37	6.5067	7.03	12
σ (dB)	4.8	4.8	4.8	4.8

Table 2: S-V model characteristics

Model Characteristics	CM 1	CM 2	CM 3	CM 4
Mean excess delay (ns)	5.2737	9.8188	15.705	22.198
RMS delay (ns)	5.5691	8.2946	14.792	19.835
NP10dB	19.3	20.65	33.69	50.84
NP (85%)	24.71	34.98	62.46	99.86

The model characteristic CM1 is based on LOS (0-4m), CM2 is based on NLOS (0-4m), CM3 is based on NLOS (4-10m) and CM4 was generated to fit a 20 ns RMS delay spread to represent an extreme multipath channel.

Simulation Results

From now on, we provide the BER performance results of the proposed differential detection with PSM and BPM signal by adjustable guard-time (data rate), in the modified S-V multipath channel.

Figure 3 and 4 illustrate the received PSM and BPM signals at the receiver data rate =25Mbps, CM1, Eb/No=30dB, $y(t)$ is the output of integrator for decision bit output. This showed the differential amplitude of BPM is longer than of PSM.

Figure 5 shows the BER performance of a differential detection with PSM versus BPM by varying channel model CM1-CM4 at data rate of 25 Mbps. While the BER performance at the data rate of 50, 100 and 150Mbps are shown in figure 6-8, respectively.

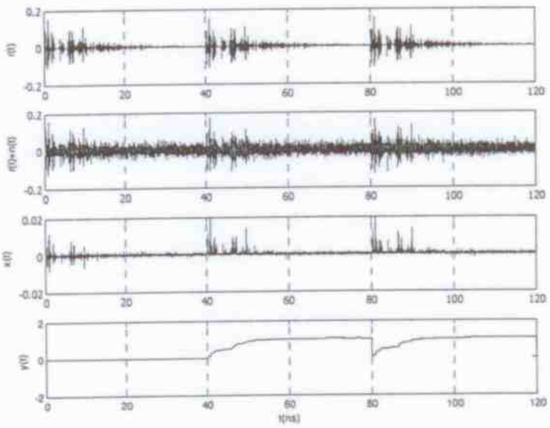

Figure 3: Received PSM signals at the receiver data rate =25Mbps, CM1, Eb/No=30dB

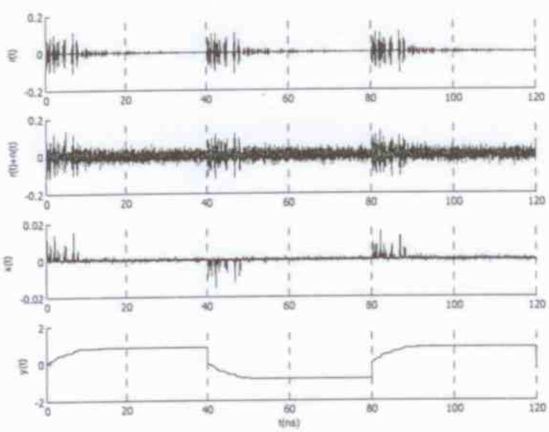

Figure 4: Received BPM signals at the receiver data rate =25Mbps, CM1, Eb/No=30dB

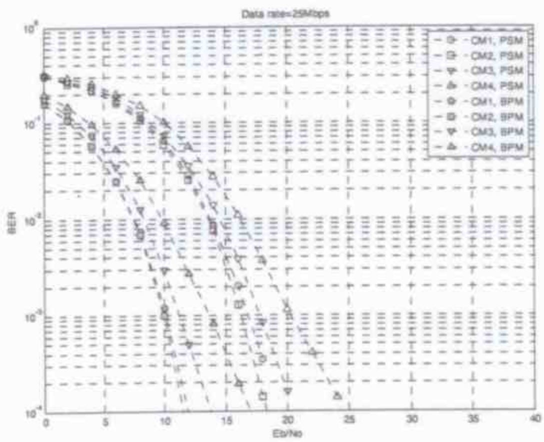

Figure 5: BER performance of PSM and BPM with data rate 25Mbps, CM1-4

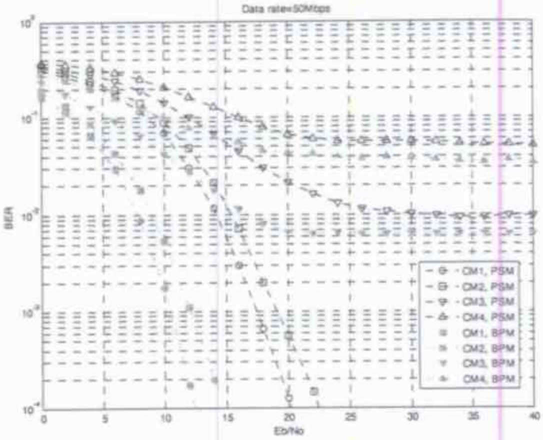

Figure 6: BER performance of PSM and BPM with data rate 50Mbps, CM1-4

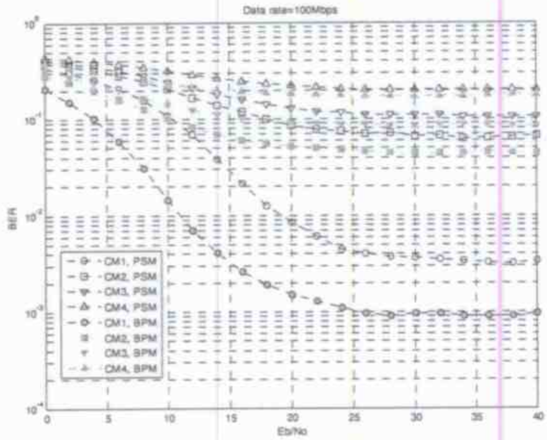

Figure 7: BER performance of PSM and BPM with data rate 100Mbps, CM1-4

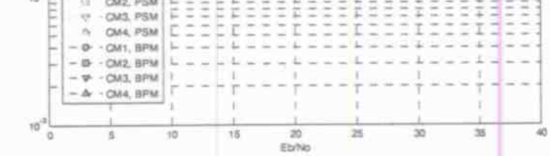

Figure 8: BER performance of PSM and BPM with data rate 150Mbps, CM1-4

Conclusions

In this paper, it was shown that the performance of differential detection with PSM versus BPM signal has been proposed for UWB indoor communication system. The BER of BPM (antipodal signal) is lower than PSM (orthogonal signal) because the BPM symbol distance between bit "0" and bit "1" is longer than PSM symbol distance 2 times.

The BER of the differential detection with BPM and PSM is depended on data rate which the low data rate has better BER than the high data rate because the ISI highly impacts in the sequence which is the lowest guard time. The simple implementation is the strong point of the differential detection which doesn't need channel estimation for equalizing UWB signal. However, the BER performance that was affected from ISI can be improved by decreasing data rate or selecting BPM for communication instead of PSM.

In the future, we intend to analyze the proposed combination between BPM and PSM for increasing data rate. It is possible to assign different pulse shapes of each M-ary for increasing the data rate with the same environment.

References

M. Ghavami, L.B.Michael and R.Kohno "Ultra Wideband Signals and Systems in Communication Engineering", Great Britain : John Wiley & Sons, Ltd. 2004.

P.Prommasuksakul, P.Supanakoon, S.Promwong and J.Takada, "Power Spectral Density Analysis of Ultra Wideband Signal Using Pulse Shape Modulation", ECTI-CON 2007. 2007, pp. 880-883.

M .Ho, V.S.Somayazulu, J.Foerster, and S.Roy, "A Differential Detector for Ultra-Wideband Communication System", IEEE. 2002, pp. 1896-1900.

J. Foerster, "UWB channel modeling sub-committee report final", IEEE P802.15 Working Group for Wireless Personal Area Networks (WPANs), Feb. 2003.

J.G.Proakis, M.Salehi and G.Bauch "Contemporary Communication Systems using MATLAB® and Simulink®. 2nd ED.", Canada : Thomson Learning, Inc. 2004.

P.Prommasuksakul, P.Supanakoon, S.Promwong and J.Takada, "Power Spectral Density of UWB PSM Signal", Thammasat Int. J. Sc. Tech., Vol. 12, No. 4, October-December2007, pp.74-80.

N.Boubaker and K.B.Letaief, "Biorthogonal Pulse Shape Modulation For Ultra-Wideband Wireless Communications", IEEE Communications Society Globecom 2004, pp.3493-3497.

L.Wu and A.Vosoughi, "Biorthogonal Pulse Shape Modulation for IR-UWB Systems over Fading Channels", SPAWC 2008. IEEE, pp. 191-195.